

ELECTROHYDRODYNAMIC RAYLEIGH-TAYLOR INSTABILITY IN A NON-NEWTONIAN FLUID LAYER BOUNDED ABOVE BY A POROUS LAYER

N. Rudraiah, Krishna B. Chavaraddi, I. S. Shivakumara & B. M. Shankar

ABSTRACT: With the growing importance of non-Newtonian fluids in modern technology and industries, investigations on such fluids are desirable. In the present paper is to study the Electrohydrodynamic Rayleigh-Taylor instability (ERTI) in a thin layer of an incompressible non-Newtonian fluid, assuming it obeys power law, confined above by a interface with a heavier fluid, and below by an impermeable rigid boundary subject to linear stability analysis. The formulation developed in the present work is to evaluate the influence of the combined effects of electric field, non-Newtonian fluid, surface tension and the layer thickness on the ERTI using the approximations described by Rudraiah *et al.*, (1996). These approximations simplify the power-law equation and pave the way to find analytical solution for velocity distribution which will be used in the dispersion relation obtained using suitable boundary and interface conditions.

Keywords: Electrohydrodynamic Rayleigh-Taylor instability (ERTI), Power-law fluid, Electric field.

NOMENCLATURE

<p>B Bond number ($\delta\lambda^2/\gamma$)</p> <p>$b(m)$ fitting constant</p> <p>C concentration</p> <p>C_0 reference concentration</p> <p>\vec{E} electric field</p> <p>\vec{g} gravitational acceleration</p> <p>h fluid film thickness</p> <p>H thickness of porous layer</p> <p>\vec{J} current density</p> <p>k_1 consistency index</p> <p>ℓ wave number</p> <p>m index parameter</p> <p>n growth rate</p> <p>P pressure</p> <p>\vec{q} velocity</p> <p>S Strouhal number (L/TU)</p> <p>U characteristic velocity</p> <p>T characteristic time ($\mu\gamma/h^3\delta^2$)</p> <p>We electric parameter ($\epsilon v_0^2/\delta h^3$)</p> <p>$x, y$ coordinates</p> <p>u, v velocity coordinates</p>	<p>Greek Symbols</p> <p>α_p slip parameter</p> <p>α_h volumetric expansion coefficient of σ</p> <p>δ drag constant</p> <p>ϵ_e dielectric constant</p> <p>ρ fluid density</p> <p>ρ_e density of charges</p> <p>s electrical conductivity</p> <p>s_p porous parameter</p> <p>μ fluid viscosity</p> <p>$\vec{\tau}_i$ stress tensor</p> <p>ϕ electric potential</p> <p>∇ differential operator</p> <p>ν kinematic viscosity (μ/ρ)</p> <p>γ surface tension</p> <p>Subscript</p> <p>f fluid</p> <p>p porous layer</p>
----------------------------------------------------------------------------------------------------------------------------------------------------------------------------------------------------------------------------------------------------------------------------------------------------------------------------------------------------------------------------------------------------------------------------------------------------------------------------------------------------------------------------------------------------------------------------------------------------------------------------------------------------------------------------------------------------------------------------------------------------------------------------------------------------------------------------------------------------------------------------------------------------------------------------------------------------------------------------------------------------------------------------------------	--------------------------------------------------------------------------------------------------------------------------------------------------------------------------------------------------------------------------------------------------------------------------------------------------------------------------------------------------------------------------------------------------------------------------------------------------------------------------------------------------------------------------------------------------------------------------------------------------------------------------------------------------------------------------------------------------------------------------------------------------------------------------------------------------------------------------------

1. INTRODUCTION

Though this topic encompasses different areas, such as space science, astrophysics and so on, its application is found mainly in solidification processes, inertial fusion energy (IFE) and cooling of machineries. So it is imperative that the present processing techniques and systems have to be modified to improve the quality of the final product. One of the most demanding engineering issues in IFE reactors is the design of a reaction chamber that can withstand the intense photons, neutrons and charged particles due to the fusion event. Rapid pulsed deposition of energy within thin surface layers of the fusion reactor components such as the first wall may cause severe surface erosion due to ablation. An innovative concept for the protection of IFE reactor cavity first walls from the direct energy deposition associated with soft X-rays and target debris is the thin liquid film protection scheme. In this concept, a thin film of molten liquid lead is fed through a silicon carbide first wall to protect it from the incident irradiations. In IFE, the hollow shells are filled with an equal mixture of Deuterium and Tritium (DT) fluid at high pressure and then solidified to the cryogenic temperature so that the DT-fluid freezes forming a thin mushy coating on the inside of the ablative surface of the shell wall. The direct-drive laser heat at this ablative surface directly causing surface instabilities.

The following different types of interfacial or surface instabilities are encountered:

- (i) Rayleigh-Taylor instability (RTI)
- (ii) Kelvin-Helmholtz Instability (KHI)
- (iii) Richtmyer-Meshkov Instability (RMI)

As discussed above the surface instabilities at target surface, there has been a considerable practical interest in the study of surface instability of the Rayleigh-Taylor type. The RTI occurs at an interface between a dense fluid supported by a less dense fluid when the latter is at high pressure. These instabilities have attracted considerable interest both theoretically (see Chandrasekhar, 1961 and Sharp, 1984) and experimentally (see Kull, 1991) because of the importance in understanding the control and exploitation of many of the basic physical, chemical and biological processes. Babchin *et al.*, (1983) have studied the non-linear RT instability in a thin Newtonian fluid film when the wavelength is much greater than the film thickness. Later, Brown (1989) relaxed this assumption on the wavelength and studied the RT instability in a finite thin layer of a viscous fluid using the combined Stokes and lubrication approximations as Babchin *et al.*, (1983). Recently, Rudraiah *et al.*, (1997, 1996) have extended the work of Brown (1989) to include the viscosity stratification and the effect of oblique magnetic field in Newtonian fluids. The works mentioned above are mainly concerned with Newtonian fluid. However, there is a rather different subject area of polymer processing applications, where, the polymers having chain molecules and behaving as a viscoelastic fluid over longer times have a range of unlikely behavior. In conditions of shear flow, they develop instabilities that of linked polymers. This failure has been shown to occur by the formation and growth of planar defects called crazes. When this crazing is accelerated by the presence of plasticizing fluid, it is likely that a thin layer of material adjacent to the heavy fluid will plasticize undergoing RTI as in the Newtonian fluid discussed by Brown (1989).

A very common technology motivation is the potential use of RTI to predict the end product in the manufacture of new materials in the material processing. Another motivation is in the area of polymer processing application to understand the knowledge of shear sensitivity of the material being processed, because excess shear to the polymer in the system may result in the structural breakdown, which in turn will have a significant effect on the mechanical properties of the final end product. The present study is also motivated to understand the elastic behaviour of fluids in biomechanics, particularly in synovial joints and in coronary arteries bounding the endothelium. The synovial fluid in the synovial joints has to maintain elasticity of the fluid to ensure low shear and to prevent the abnormal behaviour of the surface between the synovial fluid and the cartilages. Similarly in coronary artery disease, bypass surgery has been recently replaced by laser surgery. The high intensity laser no doubt dissolves plaque (i.e. growth) on the endothelium, but causes side effect by eroding the walls of the endothelium. To overcome this erosion there is a need to reduce the growth rate of this surface instability mainly of the RTI type. Usually in these biomechanical problems the physiological fluid does not behave,

except under some special situations, as Newtonian fluid instead it behaves as a non-Newtonian fluid. Therefore, to control the side effects mentioned earlier, it is essential to study RTI in non-Newtonian fluid bounded by the porous nature of endothelium.

Another example where surface instabilities play a significant role is the synovial joints which are freely movable joints. They consist of an articulate cartilage which is a two-phase deformable porous material having fixed electrical charges embedded in the tissue and a positively charged liquid (see Rudraiah *et al.*, 1998, Ng *et al.*, 2005) and the synovial fluid which is in general a non-Newtonian fluid having viscosity 1000 times that of water. One of the causes for degenerative changes in cartilages, evolving through osteoarthritis due to old age, Traumatic arthritis due to injuries, Rheumatoid arthritis due to diseases, is due to surface instabilities of the type RTI occurring at the interface between artificial cartilage and synovial fluid. Since the cartilage is a fluid saturated porous medium layer the synovial fluid, there is a need to understand the nature of surface instability at the cartilage lined with the non-Newtonian nature of synovial fluid for the effective design of artificial joints.

A great deal of research on RTI has been carried out in a Newtonian fluid. But, very little is known about RTI in a non-Newtonian fluid with application to polymer processing. As stated earlier, one of the objectives in studying the RTI in a non-Newtonian fluid has been to develop an understanding of the responses of the complex systems to various types of deformation, so that useful information is generated for practical purposes. The literature on RTI reveals that mathematical modeling of non-Newtonian fluid is very complicated and beyond the comprehension of obtaining exact solution. The experimental works in RTI pertain to simplified flow systems and situations which are too ideal and have little importance in actual practice. Therefore, with an interest for practical application, it is desirable to compromise complicated mathematical models and the pure estimates of simple experimental results leading to thumb rule formula.

The study of RT instability in non-Newtonian fluids in a finite thickness layer obeying power law viscoelastic fluid model is of considerable interest in material processing, particularly, in understanding the defects in the manufacture of new type of polymer materials used in many industrial applications. These defects are bound to occur at very low flow rates in materials having very high viscosity. The control of viscosity can be achieved with increasing rate of shear in a steady shear flow. The understanding and control of non-Newtonian power law fluid (pseudoplastic or dilatant), provides, from the technical point of view, useful information in materials processing. Recently, Rudraiah *et al.*, (2000) have studied the RTI in a finite thickness layer of a non-Newtonian fluid and they concluded that the nature of the dispersion curve is influenced by both the reciprocal of the characteristic length and the non-Newtonian parameter, with the film thickness just affecting the nature of the growth rate of instability, in the sense that an increase in film thickness increases the growth rate. Not much work has been done in non-Newtonian fluid.

To achieve this objective, this paper is planned as follows. The basic equations for poorly conducting non-Newtonian power law fluid in the presence of an electric field called EHD equations are given in section 2 with suitable approximations and boundary conditions. The dispersion relation of RTI in EHD denoted by ERTI in the presence of electric field in non-Newtonian fluid layer bounded above by a porous layer is derived in section 3. The importance of maintaining an electric potential either parallel to or opposing the direction of gravity in the control of ERTI growth rate is discussed in this section. Also we have discussed the nature of stability using complimentary Ramanujan's theory in section 4. The importance conclusions are drawn in the final section.

2. MATHEMATICAL FORMULATION

The physical configuration is shown in Fig.1. It consists of a thin target shell in the form of a thin film of unperturbed thickness h (region 1) filled with an incompressible, viscous, poorly electrically conducting non-Newtonian lighter power-law fluid of density ρ_f bounded below by a rigid surface at $y = 0$ and above by an incompressible, viscous poorly conducting non-Newtonian heavier power-law fluid of density ρ_p saturating a

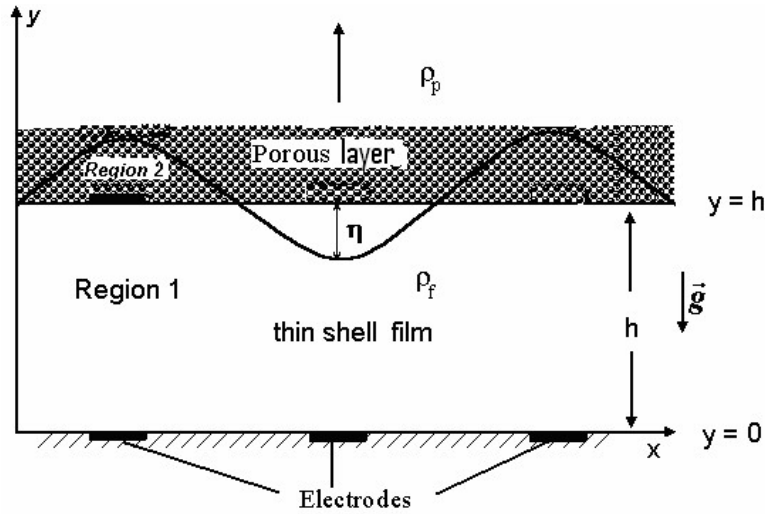


Figure 1: Physical Configuration

dense porous layer of large extent compared to the shell thickness h . Also, the electrodes are embedded at the rigid surface $y = 0$ as well as at the interface $y = h$ and there by an electric field is generated in fluid-porous medium composite system. The fluid in the thin film is set in motion by acceleration normal to the interface whereas in the porous layer it is assumed to be static and small perturbations are amplified when acceleration is directed from the lighter fluid in the thin film to the heavier fluid in the porous layer. The instability at the interface in the presence of electric field is known as electrohydrodynamic Rayleigh-Taylor instability (ERTI). To investigate this ERTI, we consider a rectangular coordinate system (x, y) with the x -axis parallel to the film and y -axis normal to it. The interface between the porous layer and thin film (fluid) is described by $\eta(x, t)$.

The basic equations for poorly electrically conducting non-Newtonian fluid in the thin film considered here are (see Rudraiah and Kaloni, 1990):

The conservation of mass:

$$\nabla \cdot \vec{q} = 0 \quad (2.1)$$

The conservation of momentum:

$$\rho \frac{D\vec{q}}{Dt} = -\nabla p + \nabla \cdot \vec{\tau} + \rho_e \vec{E} \quad (2.2)$$

The conservation of electric charges:

$$\frac{\partial \rho_e}{\partial t} + (\vec{q} \cdot \nabla) \rho_e + \nabla \cdot \vec{J} = 0 \quad (2.3)$$

The Maxwell's equations:

$$\nabla \cdot \vec{E} = \frac{\rho_e}{\epsilon_e} \quad (2.4a)$$

$$\nabla \times \vec{E} = 0 \quad \text{or} \quad \vec{E} = -\nabla \phi \quad (2.4b)$$

$$\vec{J} = \sigma \vec{E} \quad (2.4c)$$

$$\alpha = \sigma_0 [1 + \alpha_h (C - C_0)]. \quad (2.4d)$$

The physical quantities appearing in the above equations are defined in the nomenclature.

The stress tensor $\bar{\tau}_i$ expressed as

$$\bar{\tau}_i = k_1 \left\{ \frac{1}{2} \left(\frac{1}{2} \dot{\gamma}_i : \dot{\gamma}_i \right)^{\frac{m-1}{2}} \right\} \dot{\gamma} \quad (2.5)$$

where k_1 is the consistency index and $\dot{\gamma}$ is the rate of strain given by

$$\dot{\gamma}_{i,j} = \left(\frac{\partial q_i}{\partial x_j} + \frac{\partial q_j}{\partial x_i} \right) \dot{\gamma}. \quad (2.6)$$

The electrical conductivity σ varies with concentration C of deuterium-tritium as in Eq. (2.3). Then assuming negligible advection of concentration, we have

$$\frac{d^2 C}{dy^2} = 0 \quad (2.7)$$

with

$$C = C_0 \quad \text{at} \quad y = 0 \quad (2.8a)$$

$$C = C_1 \quad \text{at} \quad y = h. \quad (2.8b)$$

Solving Eq. (2.7) using the given conditions and substituting this solution in Eq.(2.4d), we get

$$\sigma = \sigma_0 [1 + \alpha y] \approx \sigma_0 e^{\alpha y} \quad (2.9)$$

where $\alpha = \alpha_h \Delta C / h$ and $\Delta C = C_1 - C_0$. We assume the frequency of charge distribution is smaller than the corresponding relaxation frequency of the electric field, and hence the time derivative of ρ_e is negligible compared to $\nabla \cdot (\sigma E)$ in Eq. (2.3). From this, we get

$$\frac{\partial^2 \phi}{\partial x^2} + \frac{\partial^2 \phi}{\partial y^2} + \alpha \frac{\partial \phi}{\partial y} = 0. \quad (2.10)$$

The above equation has to be solved subject to the boundary conditions

$$\phi = \frac{v_0 x}{h} \quad \text{at} \quad y = 0 \quad (2.11)$$

$$\phi = v_0 \frac{(x - x_0)}{h} \quad \text{at} \quad y = h. \quad (2.12)$$

These conditions arise due to embedded electrodes at $y = 0$ and $y = h$ and permits a linear variation of ϕ with x .

2.1 Assumptions and Approximations

To investigate the problem posed in this paper, following Rudraiah *et al.*, (1996), we make use of the following electrohydrodynamic approximations:

- (i) The porous medium is homogeneous, isotropic and saturated.
- (ii) The film thickness h is much smaller than the thickness H of the porous layer bounded above the film. That is,

$$h \ll H.$$

(iii) The Strouhal number S is assumed to be negligibly small.

$$S = \frac{L}{TU} \ll 1$$

The physical quantities are defined in the nomenclature.

(iv) The surface elevation η is assumed to be small compared to film thickness h . That is,

$$\eta \ll h.$$

(v) The induced magnetic field is negligible compared to the applied magnetic field since the fluid considered is poorly conducting (i.e., $\sigma \ll 1$).

Following the above assumptions and approximations (i.e., Stokes and lubrication approximations) and also assuming that the heavy fluid in the porous layer is almost static because of creeping flow approximation in a densely packed porous medium lead the basic equations in the thin film region to the following form:

$$0 = \frac{\partial u}{\partial x} + \frac{\partial v}{\partial y} \quad (2.13)$$

$$0 = -\frac{\partial p}{\partial x} + \frac{\partial}{\partial y} \left[k_1 \left| \frac{\partial u}{\partial y} \right|^{m-1} \frac{\partial u}{\partial y} \right] + \rho_e E_x \quad (2.14)$$

$$0 = -\frac{\partial p}{\partial y} + \rho_e E_y. \quad (2.15)$$

For fully developed flow, Eq. (2.10) becomes

$$\frac{\partial^2 \phi}{\partial y^2} + \alpha \frac{\partial \phi}{\partial y} = 0. \quad (2.16)$$

The solution of this equation using the boundary conditions (2.11) and (2.12) is

$$\phi = \frac{v_0}{h} \left[x - \frac{x_0}{1 - e^{-\alpha h}} (1 - e^{-\alpha y}) \right]. \quad (2.17)$$

Equations (2.4a), using Eq. (2.17), becomes

$$\rho_e = -\frac{v_0}{h} \frac{x_0 \alpha^2 e^{-\alpha y}}{1 - e^{-\alpha h}} \quad (2.18)$$

and hence

$$\rho_e E_x = -\rho_e \frac{\partial \phi}{\partial x} = \frac{v_0^2}{h^2} \frac{x_0 \alpha^2 e^{-\alpha y}}{1 - e^{-\alpha h}}. \quad (2.19)$$

3. DISPERSION RELATION

To find the dispersion relation, first we have to find the velocity distribution from Eq. (2.14) using the following boundary and surface conditions:

(i) The no-slip condition at the rigid surface:

$$u = 0 \quad \text{at} \quad y = 0. \quad (3.1)$$

(ii) The Saffman (1971) slip condition:

$$\frac{\partial u}{\partial y} = -\frac{\alpha_p}{\sqrt{k}} u \quad \text{at} \quad y = h. \quad (3.2)$$

(iii) The kinematic condition:

$$v = \frac{\partial \eta}{\partial t} \quad \text{at} \quad y = h. \quad (3.3)$$

(iv) The dynamic condition:

$$p = -\delta\eta - \gamma \frac{\partial^2 \eta}{\partial x^2} \pm \varepsilon_e \frac{E_x^2 \eta}{h} \quad \text{at} \quad y = h. \quad (3.4)$$

where physical quantities are defined in the nomenclature.

The solution of (2.14) subject to the above conditions is

$$u = \frac{1}{k_1 b(m)} \left[\frac{\partial p}{\partial x} \frac{y^2}{2} - \frac{v_0^2}{h^2} \frac{e^{-\alpha y}}{1 - e^{-\alpha h}} \right] + a_1 y + a_2 \quad (3.5)$$

where

$$a_1 = \frac{1}{k_1 b(m)} \left[\frac{1}{2} \frac{(2 + \alpha_p \sigma_p) h}{(1 + \alpha_p \sigma_p)} \frac{\partial p}{\partial x} + \frac{\alpha_p \sigma_p v_0^3}{(1 + \alpha_p \sigma_p) h^3} + \frac{v_0^2 \alpha e^{-\alpha h}}{h^2 (1 + \alpha_p \sigma_p) (1 - e^{-\alpha h})} \right]$$

$$a_2 = \frac{v_0^2}{k_1 b(m) h^2 (1 - e^{-\alpha h})}.$$

After integrating Eq. (2.13) with respect to y between $y = 0$ and h and using Eq. (3.5), we get

$$v(h) = - \int_0^h \frac{\partial u}{\partial x} dy = \frac{h^3}{12 k_1 b(m)} \frac{\partial^2 p}{\partial x^2} \left[\frac{4 + \alpha_p \sigma_p}{1 + \alpha_p \sigma_p} \right]. \quad (3.6)$$

Equation (3.3), using (3.6) and (3.4), becomes

$$\frac{\partial \eta}{\partial t} = - \frac{h^3}{12 k_1 b(m)} \left(\frac{4 + \alpha_p \sigma_p}{1 + \alpha_p \sigma_p} \right) \left[\left(\delta \pm \frac{\varepsilon_e E_x^2}{h} \right) \frac{\partial^2 \eta}{\partial x^2} + \gamma \frac{\partial^4 \eta}{\partial x^4} \right]. \quad (3.7)$$

To investigate the growth rate, n of the periodic perturbation of the interface, we look for the solution of Eq. (3.7) in the form

$$\eta = \eta(y) \exp \{i\ell x + nt\} \quad (3.8)$$

where the physical quantities are defined in the nomenclature.

Substituting Eq. (3.8) into (3.7), we obtain the following dispersion relation

$$n = - \frac{h^3}{12 k_1 b(m)} \left(\frac{4 + \alpha_p \sigma_p}{1 + \alpha_p \sigma_p} \right) \left[- \left(\delta \pm \frac{\varepsilon_e v_0^2}{h^2} \right) \ell^2 + \gamma \ell^4 \right]. \quad (3.9)$$

Making Eq. (3.9) dimensionless using the quantities

$$n^* = \frac{nk_1}{\sqrt{\gamma\delta}}, \quad h^* = \frac{h}{\sqrt{\gamma\delta}}, \quad \ell^* = \ell\sqrt{\gamma/\delta}, \quad v^* = \frac{v_0}{h} \quad (3.10)$$

we obtain

$$n = \frac{h^3 \ell^2}{12b(m)} \left(\frac{4 + \alpha_p \sigma_p}{1 + \alpha_p \sigma_p} \right) \left[(1 \pm We) - \frac{\ell^2}{B} \right] \quad (3.11)$$

where the physical quantities are defined in the nomenclature and We is the electric parameter physically represents the measure of electric energy to pressure energy, $b(m)$ is a fitting constant and B is the Bond number measures the relative importance of gravitational force to surface tension. The positive or negative sign in front of We in the above equation will depend on whether the potential difference is along or opposing the gravity. Since the potential difference is opposing the gravity, we have chosen the negative sign and Eq. (3.11) takes the form

$$n = \frac{h^3 \ell^2}{12b(m)} \left(\frac{4 + \alpha_p \sigma_p}{1 + \alpha_p \sigma_p} \right) \left[(1 - We) - \frac{\ell^2}{B} \right]. \quad (3.12)$$

This is the required dispersion relation. From this dispersion relation we recover the results of Rudraiah *et al.*, (2007) for Newtonian fluid if $b(m) = 1$ for $m = 1$. Also, this result coincides with Rudraiah (2003) if $b(m) = 1$, $We = 0$ and $h = 1$. Thus the fitting constant $b(m)$ should be chosen in such a way that $b(1) = 1$. Thus we consider the following cases for discussion

Case (i): $b(m) = \frac{m+1}{2}$.

Case (ii): $b(m) = \frac{1}{2} + \frac{m}{4} + \frac{m^2}{4}$.

The dispersion relation (3.12) is computed for different values of m , We , B and σ_p suitable for shear thinning and shear thickening flows and the results are shown in Figs. 5-14 for the above two cases.

Setting $n = 0$ in Eq.(3.12), we obtain the cut-off wave number, ℓ_{ct} in the form

$$\ell_{ct} = \sqrt{B(1 - We)}. \quad (3.13)$$

The maximum wave number, ℓ_m obtained from Eq. (3.12) by setting $\partial n / \partial \ell = 0$ is

$$\ell_m = \sqrt{\frac{B(1 - We)}{2}} = \frac{\ell_{ct}}{\sqrt{2}}. \quad (3.14)$$

We note that in the case of applied voltage opposing the gravity ℓ_{ct} and ℓ_m are real only if $We \leq 1$. However, in the case of applied voltage in the direction of gravity we get $1 + We$ in Eqs. (3.13) and (3.14) and hence in that situation ℓ_{ct} and ℓ_m are real for all values of We .

The corresponding maximum growth rate, n_m for applied voltage opposing the gravity is

$$n_m = \frac{h^3 B}{48b(m)} \left(\frac{\alpha_p \sigma_p + 4}{\alpha_p \sigma_p + 1} \right) (1 - We)^2. \quad (3.15)$$

This growth rate n_m will be zero for $We = 1$. Physically this implies the equi-partition of energy (i.e., electric energy balances with pressure energy. Since pressure has the dimension of kinetic energy, this equi-partition can also be stated as electric energy balances with kinetic energy). If we choose the voltage such that $We = 1$, asymmetry can be completely reduced and hence maximum efficiency of IFE may be achieved.

Similarly, the maximum classical growth rate, n_{bm} , for $\sigma_p = 0$, $We = 0$ using $\ell_m = \sqrt{B/2}$, is given by

$$n_{bm} = \frac{B}{12} \tag{3.16}$$

Therefore,

$$G_m = \frac{n_m}{n_{bm}} = \frac{h^3}{4b(m)} \left(\frac{\alpha_p \sigma_p + 4}{\alpha_p \sigma_p + 1} \right) (1 - We)^2. \tag{3.17}$$

To know the reduction in growth rate of the IFE target, the above analytical expression for G_m is computed for different values of m by fixing $We = 0.25$, $\sigma_p = 4$ and $\alpha_p = 0.1$ and the results are tabulated in Table 1. The growth rate given by Eq. (3.12) is also computed numerically for different values of parameters and the results are presented graphically in Figs.5 -14.

For case (i): $b(m) = \frac{m+1}{2}$

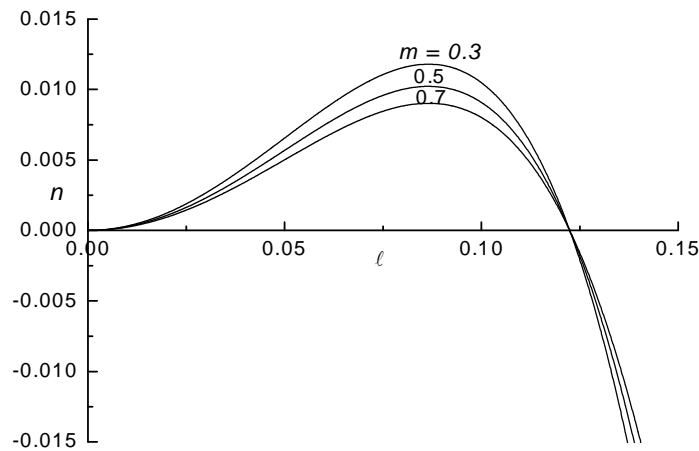


Figure 2: Growth Rate, versus the Wave Number, ℓ for Different Values of Power-Law Index m when $h = 5$, $\alpha_p = 0.1$, $\sigma_p = 4$, $B = 0.02$ and $We = 0.25$

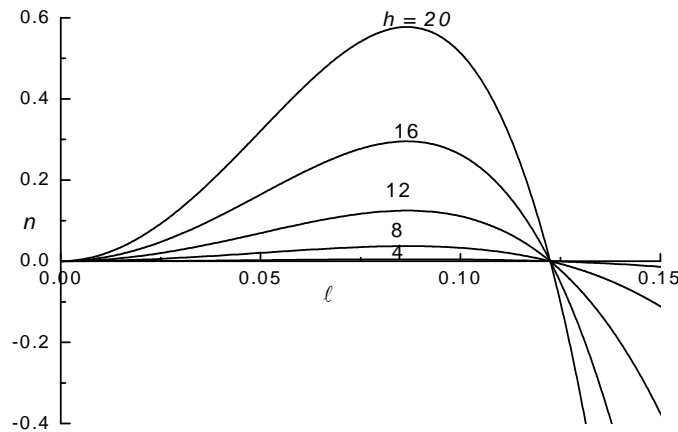


Figure 3: Growth Rate, versus the Wave Number, ℓ for Different Values of Thickness Parameter h when $m = 0.5$, $\alpha_p = 0.1$, $\sigma_p = 4$, $B = 0.02$ and $We = 0.25$

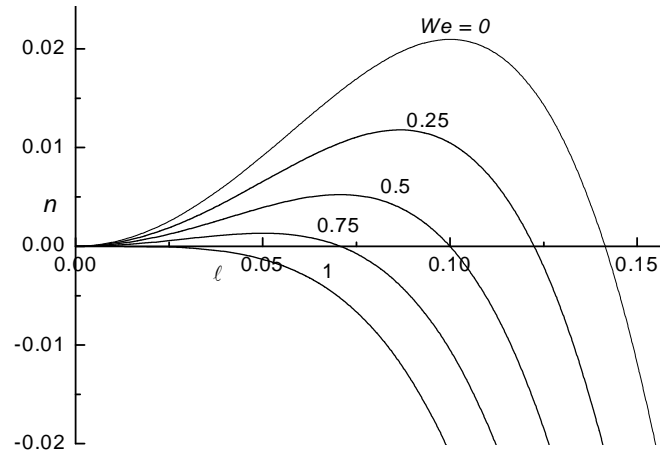


Figure 4: Growth Rate, n versus the Wave Number, ℓ for Different Values of Electric Parameter, We when $h = 5$, $m = 0.5$, $\alpha_p = 0.1$, $\sigma_p = 4$ and $B = 0.02$

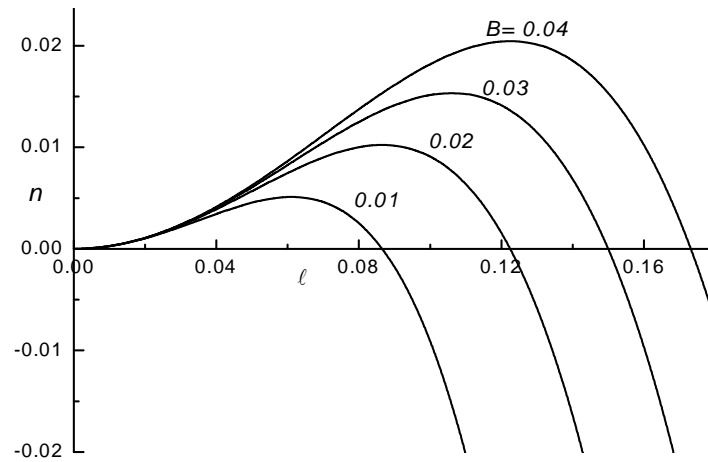


Figure 5: Growth Rate, n versus the Wave Number, ℓ for Different Values of Bond Number, B when $h = 5$, $m = 0.5$, $\alpha_p = 0.1$, $\sigma_p = 4$ and $We = 0.25$

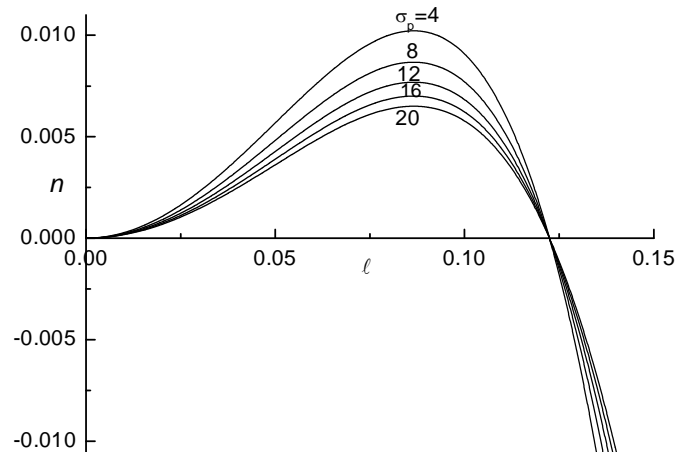


Figure 6: Growth Rate, n versus the Wave Number, ℓ for Different Values of Porous Parameter σ_p when $h = 5$, $m = 0.5$, $\alpha_p = 0.1$, $B = 0.02$ and $We = 0.25$

For Case (ii) :
$$b(m) = \frac{1}{2} + \frac{m}{4} + \frac{m^2}{4}$$

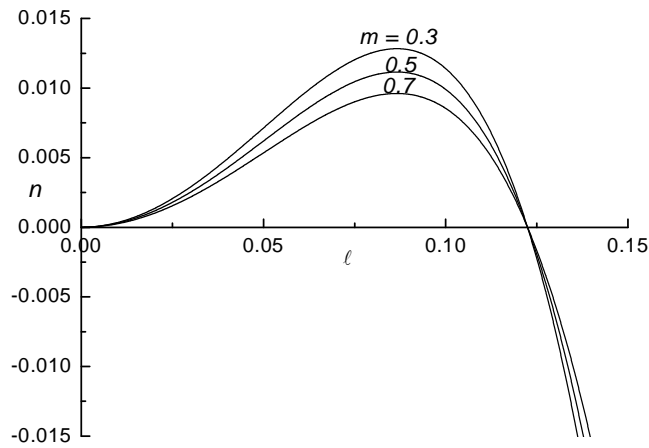


Figure 7: Growth Rate, n versus the Wave Number, ℓ for Different Values of Power-Law Index m when $h = 5$, $\alpha_p = 0.1$, $\sigma_p = 4$, $B = 0.02$ and $We = 0.25$

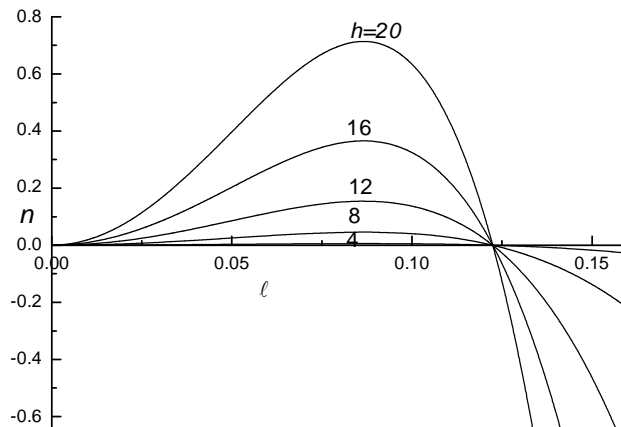


Figure 8: Growth rate, n versus the wave number, ℓ for Different Values of Thickness Parameter h when $m = 0.5$, $\alpha_p = 0.1$, $\sigma_p = 4$, $B = 0.02$ and $We = 0.25$

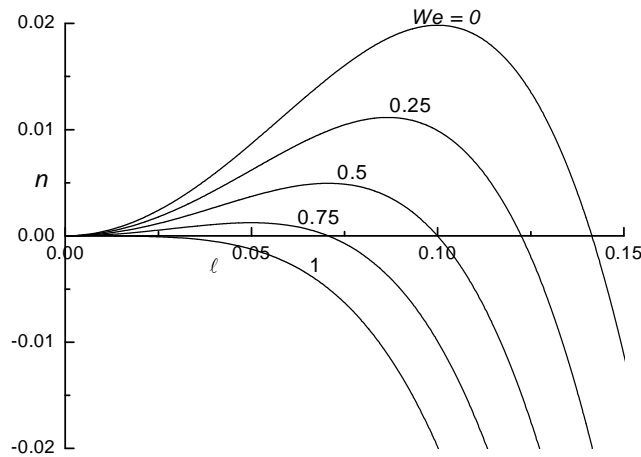


Figure 9: Growth Rate, n versus the Wave Number, ℓ for Fiffereent Values of Electric Parameter We when $h = 5$, $m = 0.5$, $\alpha_p = 0.1$, $B = 0.02$ and $\sigma_p = 4$

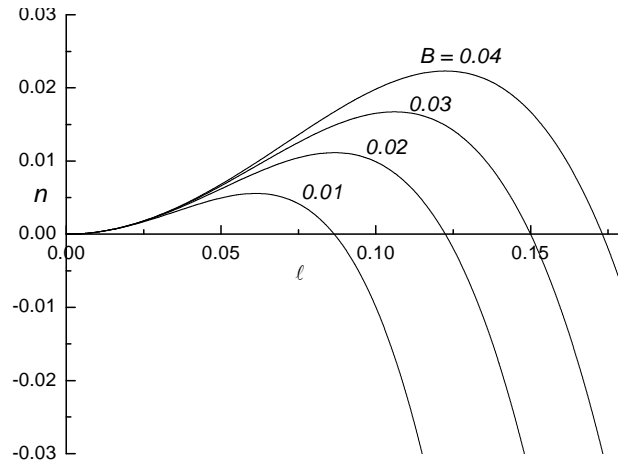


Figure 10: Growth Rate, n versus the Wave Number, ℓ for Different Values of Bond Number B when $h = 5$, $m = 0.5$, $\alpha_p = 0.1$, $\sigma_p = 4$ and $We = 0.25$

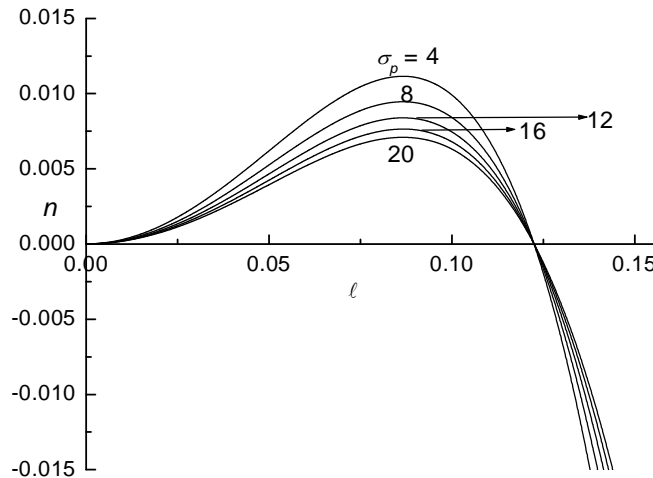


Figure 11: Growth Rate, n versus the Wave Number, ℓ for Different Values of Porous Parameter, σ_p when $h = 5$, $m = 0.5$, $\alpha_p = 0.1$, $B = 0.02$ and $We = 0.25$

5. RESULTS AND DISCUSSION

The linear electrohydrodynamic Rayleigh-Taylor instability (ERTI) in a power-law fluid layer bounded above by a porous layer and below by a rigid surface in the presence of electric field is investigated. To know the extent of reduction in the asymmetry of the RTI at the interface, the ratio of growth rate G_m is computed by Eq. (3.17) for different values of power-law index m and the results are tabulated in Table 1.

From this table, it is clear that the power-law index m has stabilizing influence on the instability of the plane interface between the composite fluid-porous layer system in the presence of electric field and surface tension. It is seen that there is 85% reduction of ratio of growth rate for Case(i) and 92% reduction for Case (ii) when $m = 3$, $h = 5$, $\alpha_p = 0.1$, $\sigma_p = 4$ and $We = 0.25$. From this we conclude that with a proper choice of power-law index m , it is possible to control the growth rate of RTI and as such this is more effective than the Newtonian fluid (Rudraiah *et al.*, 2009).

Regarding the influence of power-law index m , it is noted that stable, marginally stable or unstable nature of the system will depend on the value of power-law index m . The dispersion relation is computed numerically for different values of power-law index m , We , σ_p , B , film thickness h , and wave number ℓ fixing $\alpha_p = 0.1$

Table 1
Reduction in Growth Rate for Different Values of m

Authors	G_m	Percentage of reduction in growth rate
Takabe <i>et al.</i> , (1985)	0.45	45% (for compressible fluid)
Rudraiah (2003)	0.79	79% ($\alpha_p = 0.1, \sigma_p = 4$) (for incompressible fluid with porous lining)
Rudraiah <i>et al.</i> , (2009)	0.64	64% ($B = 0.02, \alpha_p = 0.1, \sigma_p = 4, We = 0.1$) (For EHD with porous lining)
Present paper		
Case (i): $b(m) = \frac{m+1}{2}$	0.85	85% ($h = 5, \alpha_p = 0.1, \sigma_p = 4, We = 0.25, m = 0.3$)
	0.74	74% ($h = 5, \alpha_p = 0.1, \sigma_p = 4, We = 0.25, m = 0.5$)
	0.65	65% ($h = 5, \alpha_p = 0.1, \sigma_p = 4, We = 0.25, m = 0.7$)
Case (ii): $b(m) = \frac{1}{2} + \frac{m}{4} + \frac{m^2}{4}$	0.924	92% ($h = 5, \alpha_p = 0.1, \sigma_p = 4, We = 0.25, m = 0.3$)
	0.804	80% ($h = 5, \alpha_p = 0.1, \sigma_p = 4, We = 0.25, m = 0.5$)
	0.693	69% ($h = 5, \alpha_p = 0.1, \sigma_p = 4, We = 0.25, m = 0.7$)

and results are presented graphically in Figs. 2-11. It is found that the nature of dispersion relation is influenced by both the reciprocal of the characteristic length δ/γ and the power-law index m . That is, increase in the power-law index m decreases the growth rate as shown in Figs. 2 and 7 for both the cases of $b(m)$ considered with fixed $h = 5, B = 0.02, \alpha_p = 0.1, \sigma_p = 4$ and $We = 0.25$. The increase in the film thickness parameter h increases the growth rate as shown in Figs. 3 and 8 for both cases of $b(m)$ with fixed $B = 0.02, m = 0.5, \alpha_p = 0.1, \sigma_p = 4$ and $We = 0.25$. From Figs. 4 and 9, it is clear that the decrease in growth rate compared to the classical growth rate is very steep for We in the range 0.5 to 1.0 when $B = 0.02, m = 0.5, \alpha_p = 0.1, \sigma_p = 4$ and $h = 5$. Figures 5 and 10 show the variation of the Bond number, B with fixed $h = 5, m = 0.5, \alpha_p = 0.1, \sigma_p = 4$ and $We = 0.25$ and found that the perturbations of the interface having ℓ smaller than the critical wave number ℓ_{cr} are amplified when $\delta > 0$ (i.e., $\rho_f < \rho_p$) and the growth rate decreases with decrease in B . Hence, the Bond number B being the reciprocal of surface tension implies that an increase in surface tension decreases the growth rate and hence makes the interface more stable. Also, relation (3.12) is plotted in Figs. 6 and 11 for the growth rate n versus the wave number ℓ for different values of porous parameter σ_p for $h = 5, m = 0.5, \alpha_p = 0.1, B = 0.02$ and $We = 0.25$. These figures show that decrease in the growth rate compared to the classical growth rate is very steep for different values of the porous parameter σ_p in the range of 4 to 20. The effect of increase in σ_p has stabilizing effect on the growth rate of RTI.

ACKNOWLEDGEMENT

The work supported by ISRO under the research projects no. ISRO/RES/2/338/2007-08 & ISRO/RES/2/335/2007-08. ISRO's financial support to carry out this research is gratefully acknowledged. One of us (KBC) wishes to thank the Principal, Government First Grade College, Yellapur (U.K) for their encouragement and support and B.M.S gratefully acknowledges ISRO for providing JRF under the above projects.

REFERENCES

- [1] Saffman P. G., (1971), On the Boundary Condition at the Surface of a Porous Medium, *Studies in Appl. Math.*, **50**, 93.
- [2] Rudraiah N., (2003), Effect of Porous Lining on Reducing the Growth Rate of Rayleigh-Taylor Instability in the Inertial Fusion Energy Target, *Fusion Sci. and Tech.*, **43**, 1-5.
- [3] Chandrasekhar S., (1961), *Hydrodynamic and Hydromagnetic Stability*, Oxford University Press, Oxford.
- [4] Kull H. J., (1991), Theory of Rayleigh-Taylor Instability, *Phys. Report*, **206**, 198.

- [5] Mikaelian K. O., (1993), Effect of Viscosity on Rayleigh-Taylor and Richtmyer-Meshkov Instabilities, *Phys. Rev. E*, **47**, 375.
- [6] Rudraiah N., Krishnamurthy B. S., and Mathad R. D., (1996), The Effect of Oblique Magnetic Field on the Surface Instability of a Finite Conducting Fluid Layer, *Acta, Mech.*, **119**, 165.
- [7] Takabe H., Mima K., Montierth L, and Morse R. L., (1985), Self Consistent Growth Rate of the Rayleigh-Taylor Instability in an Ablatively Accelerating Plasma, *Phys. Fluids*, **28**(12), 3676.
- [8] Babchin A. J., Frenkel A. L., Levich B. G., and Shivashinsky G. I., (1983), Nonlinear Saturation of Rayleigh-Taylor Instability in Thin Films, *Phys. Fluids*, **26**, 3159.
- [9] Rudraiah N., Krishnamurthy B. S., Jalaja A. S., and Desai T., (2004), Effect of a Magnetic on the Growth Rate of Rayleigh-Taylor Instability of a Laser Accelerated Thin Ablative Surface, *Laser and Particle Beams*, **22**, 1.
- [10] Rudraiah N., Wagner C., Evans G. S., and Friedrich R., (1998), Nonlinear Study of Rayleigh-Taylor Instability in Thin Films Past a Porous Layer, *Indian J. Pure Appl. Math.*, **29**(4), 417.
- [11] Rudraiah N., Shivakumara I. S., and Krishna B. Chavaraddi, (2009), Electrohydrodynamic Rayleigh-Taylor Instability in a Poorly Conducting Fluid Layer Bounded Above by a Nanostructural Porous Layer, *Int. J. Fluid Mech. Res.*, **36**(2), 166.
- [12] Brown H. C., (1989), Rayleigh-Taylor Instability in a Finite Thickness Layer of a Viscous Fluid, *Phys. Fluid A*, **1**(5), 895.
- [13] Rudraiah N., and Kaloni P. N., (1990), Flow of Non-Newtonian Fluids, *Encyclopaedia of Fluid Mechanics*, Gulf Publishing Company, USA. **Chapter 1**, 9, 1.
- [14] Sharp D. H., (1984), An Over View of Rayleigh-Taylor Instability, *Physica D*, **12**, 3.
- [15] Ng C. O., Rudraiah N., Nagaraj C., and Nagaraj H. N., (2005), Electrohydrodynamic Dispersion of Macromolecular Components in Nanostructured Biological Bearing, *J. of Energy, Heat Mass Transfer*, **27**, 39.

N. Rudraiah, I. S. Shivakumara & B. M. Shankar

UGC-Centre for Advanced Studies in Fluid Mechanics,

Department of Mathematics, Bangalore University,

Bangalore-560 001, India.

E-mail: rudraiahn@hotmail.com

Krishna B. Chavaraddi

Department of Mathematics

Government First Grade College, Yellapur (U.K)-581 359, India.

E-mail: ckrishna2002@yahoo.com